Physically-based Assessment of Hurricane Surge Threat under Climate Change

Ning Lin[1*], Kerry Emanuel[1], Michael Oppenheimer[2], Erik Vanmarcke[3]

[1]Department of Earth, Atmospheric, and Planetary Sciences, Massachusetts Institute of Technology, Cambridge, MA 02139-4307, USA

[2]Department of Geosciences and the Woodrow Wilson School, Princeton University, Princeton, NJ 08544, USA

[2]Department of Civil and Environmental Engineering, Princeton University, Princeton, NJ 08544, USA

[*]Corresponding author, ninglin@mit.edu

Abstract

Storm surges are responsible for much of the damage and loss of life associated with landfalling hurricanes. Understanding how global warming will affect hurricane surge thus holds great interest. As general circulation models (GCMs) cannot simulate hurricane surges directly, we couple a GCM-driven hurricane model with hydrodynamic models to simulate large numbers of synthetic surge events under projected climates and assess surge threat, as an example, for New York City (NYC). Struck by several intense hurricanes in recorded history, NYC is highly vulnerable to storm surges. We show that the surge level for NYC will likely increase due to the change of storm climatology with a magnitude comparable to the projected sea-level rise (SLR), based on some GCMs. The combined effects of storm climatology change and a 1-m SLR may cause the current NYC 100-year surge flooding to occur every 3-20 years and the 500-year flooding to occur every 25-240 years by the end of the century.

Introduction

Associated with extreme winds, rainfall, and storm surges, tropical cyclones present major hazards for coastal areas. Moreover, tropical cyclones respond to climate change[1, 2, 3]. Previous studies predicted an increase in the global mean of the maximum winds and rainfall rates of tropical cyclones in a warmer climate[4]; however, the effect of climate change on storm surges, the most damaging aspect of tropical cyclones, remains to be investigated[4]. Hurricane Katrina of 2005, the costliest natural disaster in U.S. history, produced the greatest coastal flood heights ever recorded in the U.S., causing more than $100 billion in losses and resulting in about 2000 fatalities. On the eastern U.S. coast, where tropical cyclones are less frequent than in the Gulf of Mexico and Florida regions, the Great Hurricane of 1938 produced record flood heights in Long

Island and southern New England, killing 600-800 people. A question of increasing concern is whether such devastating surge events will become more frequent.

The storm surge is a rise of water driven by a storm's surface wind and pressure gradient forces over a body of shallow water; its magnitude is determined, in a complex way, by the characteristics of the storm plus the geometry and bathymetry of the coast. As a result, the change of surge severity cannot be inferred directly from the change of storm intensity [5, 6, 7, 8]. For example, Hurricane Camille of 1969 (Category 5) made landfall in the same region of Mississippi as the less intense Hurricane Katrina (Category 3), but produced lower surges due to its smaller size[5,6,9]. Using only a storm's landfall characteristics to predict surges is also inaccurate[10, 11], as the evolution of the storm before and during landfall affects the surge. Furthermore, similar storms can produce quite different surges at locations with different topological features[6]. Therefore, quantifying the impact of climate change on hurricane surges requires explicit modeling of the development of storms and induced surges at local scales under projected climates.

Modeling hurricane surges under climate scenarios, however, is not straightforward, because tropical cyclones cannot be resolved in current GCMs due to their relatively low resolution (~100 km) compared to the size of storm core (~ 5 km). Although high-resolution regional models (e.g., refs 12 and 13) may be used to downscale the GCM simulations, these models are still limited in horizontal resolution and are too expensive to implement for risk assessment. This study takes a more practical approach, coupling a simpler GCM-driven statistical/deterministic

hurricane model with hydrodynamic surge models to simulate cyclone surges for different climates.

Computationally efficient, this method can be used to generate large numbers of synthetic surge events at sites of interest, providing robust statistics to characterize surge climatology and extremes. We apply this method to investigate current and future hurricane surge threat for NYC, considering also the contribution of wave setup, astronomical tides, and SLR. The resulting surge flood return-level curves provide scientific bases for climate adaptation and sustainable development in rapidly developing coastal areas[14,15,16].

Storm simulation

The statistical/deterministic hurricane model[17, 18] used in this study generates synthetic tropical cyclones under given large-scale atmospheric and ocean environments, which may be estimated from observations or climate modeling. This method does not rely on the limited historical track database, but rather generates synthetic storms that are in statistical agreement with observations[17], and it compares well with various other methods used to study the effects of climate change on tropical cyclones[18, 19,4]. In this study, we assume the cyclone-threatened area for NYC to be within a 200-km radius from the Battery (74.02 W, 40.9 N; chosen as the representative location for NYC), and we call it a NY-region storm if a storm ever passes within this threatened area with a maximum wind speed greater than 21 m/s. To investigate the current surge probabilities, we generate a set of 5000 NY-region storms under the observed climate (represented by 1981-2000 statistics) estimated from the National Center for Environmental Prediction/National Center for Atmospheric Research (NCAR/NCEP) reanalysis[20]. To study the

89 impact of climate change, we apply each of four climate models, CNRM-CM3 (Centre National
90 de Recherches Météorologiques, Météo-France), ECHAM5 (Max Planck Institution), GFDL-
91 CM2.0 (NOAA Geophysical Fluid Dynamics Laboratory), and MIROC3.2
92 (CCSR/NIES/FRCGC, Japan), to generate four sets of 5000 NY-region storms under current
93 climate conditions (1981-2000 statistics) and another four sets of 5000 NY-region storms under
94 future climate conditions (2081-2100 statistics) for the IPCC-AR4 A1B emission scenario[21].
95 (Most of the climate data are obtained from the World Climate Research Program (WCRP) third
96 Climate Model Intercomparison Project (CMIP3) multimodel dataset.) We choose these four
97 climate models because, based on the study of ref. 18, the predictions of the changes in storm
98 frequency, intensity, and power dissipation in the Atlantic basin by these models span the range
99 of predictions by all seven CMIP3 models from which the required model output is available.
100
101 The annual frequency of the historical NY-region storms is estimated from the best-track
102 Atlantic hurricane dataset (updated from ref. 22) to be 0.34; we assume this number to be the
103 storm annual frequency under the current climate. Since the hurricane model does not produce an
104 absolute rate of genesis, the storm frequency derived from each climate model for the current
105 climate is calibrated to the observed value (0.34), and the frequency for the future climate is then
106 predicted[18]. Estimated annual frequencies of future NY-region storms from the four climate
107 models differ: CNRM is 0.7, ECHAM is 0.3, GFDL is 1.34, and MIROC is 0.29; the change of
108 the storm frequency due to global warming ranges from a decrease of 12% to an increase of
109 290%. The large variation among the model predictions reflects the general uncertainties in
110 climate models' projections of tropical cyclone frequency, due to systematic model differences
111 and internal climate variability (which may not be averaged out over the 20-yr periods

112 considered here[18]). According to ref. 23, as much as half of the uncertainty may be owing to the
113 climate variability. Moreover, the variations in the projected storm frequency changes at global
114 or basin scales, as in refs. 4 and 18, are greatly amplified at local scales, as in this study, due to
115 the differences in the storm track and intensity changes predicted by the climate models. We also
116 note that even larger variations in the storm frequency changes can be induced if more climate
117 models are considered; for example, the Hadley Center UK Meteorological Office model
118 UKMO-HadCM3 may predict a relatively large reduction in the storm frequency due to climate
119 change, based on the study of ref. 3.
120
121 ## Surge modeling
122 This study uses two hydrodynamic models: the Advanced Circulation Model (ADCIRC [24, 25])
123 and the Sea, Lake, and Overland Surges from Hurricanes (SLOSH[26]) model, both of which have
124 been validated and applied to simulate storm surges and make forecasts for various coastal
125 regions (e.g., refs 27, 28, 29, 30, 31, 32). Storm surges are driven by storm surface wind and
126 sea-level pressure fields. For the ADCIRC simulations, the surface wind (10-min. average at 10
127 m) is estimated by calculating the wind velocity at the gradient height with an analytical
128 hurricane wind profile[33], translating the gradient wind to the surface level with a velocity
129 reduction factor (0.85[34]) and an empirical expression of inflow angles[35], and adding a fraction
130 (0.5; based on observed statistics) of the storm translation velocity to account for the asymmetry
131 of the wind field; the surface pressure is estimated from a parametric pressure model[36]. For the
132 SLOSH simulations, the wind and pressure are determined within the SLOSH model by a semi-
133 parametric hurricane model[26]. The two hydrodynamic models are applied with numerical grids of
134 various resolutions (from ~1 km to ~ 10 m around NYC). The SLOSH simulation with a coarse

resolution grid is used to select the extreme surge events, which are further analyzed with higher-resolution ADCIRC simulations to estimate the probability distributions of NYC surges (see Methods and Supplementary Figs. S1 and S2).

As examples, Figure 1 displays the spatial distribution of the storm surge around the NYC area for two worst-case scenarios for the Battery under the NCAR/NCEP current climate. The storm that generates the highest surge (4.75 m) at the Battery moves northeastward and close to the site with a high intensity (Fig. 1a). A relatively weaker storm that moves farther from the site also produces a comparable surge (4.57 m) at the Battery, due to its larger size and northwestward translation (Fig. 1b). Both storms pass to the west of the Battery, inducing high surges at the site with their largest wind forces to the right of the track; this effect (of the wind field's asymmetry) on the surge is particularly significant for northwestward-moving storms, which concentrate their strongest wind forces on pushing water into New York Harbor and up to lower Manhattan. These two worst-case surges for the Battery have very low occurrence probabilities under the current climate condition. However, NYC has indeed been affected by numerous intense storm surges in recorded history and, based on the local sedimentary evidence, prehistory[37]. The highest water level at the Battery as inferred from historic archives was about 3.2 m relative to the modern mean sea level, due to a hurricane in 1821 striking NYC at a low tide[37]; thus the largest historical surge at the Battery might be about 3.8 m (given the magnitude of the local low tide of about 0.5-0.8 m).

We also investigate the influences of other processes related to the surge for NYC, using a set of over 200 most extreme surge events. To investigate the effects of wave setup, we simulate the

158 extreme events with the ADCIRC model coupled with a wave model[32]; the wave setup is found
159 to be relatively small for the study region (see Fig. S3), and thus it is neglected in our estimation
160 of surge probabilities. We notice, however, that the nonlinear effect of the astronomical tide on
161 the surge (tide-surge nonlinearity) is relatively large (see Fig. S4). We model this nonlinearity as
162 a function of the surge and tidal characteristics, based on a database generated for the extreme
163 events (see Methods and Fig. S5). This function is then used to estimate the storm tide as a
164 combination of the surge and astronomical tide. In addition, we study the nonlinear effect on the
165 surge from the SLR, by simulating the extreme surges for a range of projected SLRs for NYC.
166 This SLR effect is found to be negligible (see Fig. S6), and thus projected SLRs in future
167 climates are accounted for linearly in the estimation of the flood height for NYC.
168
169 ## Statistical analysis

170 We assume the annual number of NY-region storms to be Poisson-distributed (see Fig. S7), with
171 as mean the annual storm frequency. For each storm arrival, the probability density function
172 (PDF) of the induced surge is estimated from the generated surge database. Our empirical
173 datasets show that the surge PDF is characterized by a long tail, which determines the risk. We
174 apply a Peaks-Over-Threshold (POT) method to model this tail with a Generalized Pareto
175 Distribution (GPD), using the maximum likelihood method, and the rest of the distribution with
176 non-parametric density estimation. The GPD fits relatively well with the surge distribution for
177 almost all storm sets in this study (Figs. S8 and S9). The estimated storm frequency and surge
178 PDF are then combined to generate the surge return-level curves and associated statistical
179 confidence intervals (calculated with the Delta method[38]). The surge PDF is further applied to
180 estimate the storm tide and flood height return levels (see Methods).

Current surge threat

The estimated return levels of the storm surge at the Battery under the NCAR/NCEP current climate appear in Fig. 2. The estimated current 50-year storm surge is about 1.24 m, the 100-year surge is about 1.74 m, and the 500-year surge is about 2.78 m. A previous study[39], using the SLOSH model with a relatively coarse mesh, predicted a higher surge (2.14 m) for the 100-year return period but lower surges for longer return periods (e.g., 2.73 m for the 500-year surge) for this site. These differences result mainly from the different wind profiles and grid resolutions applied in the ADCIRC and SLOSH simulations and the different storm sets (statistical samples) used. The estimated return level of the storm tide, shown also in Fig. 2, is about 0.3-0.5 m higher than the storm surge level. Thus, the estimated current 50-year storm tide is about 1.61 m, the 100-year storm tide is about 2.03 m, and the 500-year storm tide is about 3.12 m. Considering that much of the seawall protecting lower Manhattan is only about 1.5 m above the mean sea level[30], NYC is presently highly vulnerable to extreme hurricane-surge flooding. For return periods under 50 years, extratropical cyclones may also contribute to the coastal flooding risk and become the main source of 1-10 year coastal floods for NYC[40, 41].

Impact of climate change

The predictions of storm tide return levels for current and future IPCC A1B climates are presented in Fig. 3. (In the context of climate change, the return level at period T may be understood as the level with an annual exceedance probability of $1/T$.) The results from the four climate models differ: CNRM predicts an increase of the storm tide level, while ECHAM

predicts a decrease; GFDL predicts that the storm tide level will increase for the main range of the return period but decrease for very long return periods, while MIROC predicts a decrease for low and moderate return periods but an increase for longer return periods. However, the magnitudes of the changes (the ratio of A1B to the current-climate levels) using CNRM (1.13-1.24) and GFDL (0.98-1.44) are more significant than those using ECHAM (0.89-0.96) and MIROC (0.89-1.08). The discrepancies among the model results can be attributed to the models' different estimations of the change of the storm frequency and the surge severity. The storm frequency on a local scale plays an important role in determining the surge risk; the prediction of the frequency change for NY-region storms by the four climate models varies greatly. Moreover, unlike the average storm intensity, which is predicted to increase by these and other climate models[4], the storm surge severity is predicted to increase by some models but decrease by others. This difference appears because the surge magnitude depends on other parameters of the storm as well as on its intensity, all of which may change differently in the different climate models.

We suspect that a main reason that the increase of storm intensity (in some models) does not translate to an increase in surge magnitude is that the storm's radius of maximum wind (R_m) tends to decrease as the storm intensity increases, given the assumption made in the above simulations that the distribution of the storm's outer radius (R_o, determined from observed statistics[42]) remains the same under different climates. However, in theory the storm's overall dimension scales linearly with the potential intensity[43]; therefore, the increase of potential intensity in a warmer climate[44] may induce an increase of R_o. Consequently, the reduction of R_m due to the increase of storm intensity may be offset and even reversed. In such a case, climate change will likely increase storm intensity and size simultaneously, resulting in a significant

intensification of storm surges. In order to test this hypothesis, we performed the simulations as before but assumed that R_o increases by 10% and R_m increases by 21% in the future climate. We base this assumption on the estimated change of the potential intensity in the future climate (expected to increase by about 10%[4]) and on a theoretical scaling relationship between R_o and R_m (R_m scales with R_o^2)[33]. The storm tide level thus predicted, shown also in Fig. 3, is higher or nearly unchanged in the future climate for the four models. The magnitude of the change also grows due to the increase of the storm size; it becomes 1.23-1.36 for CNRM, 1.05-1.50 for GFDL, 0.95-1.02 for ECHAM, and 0.97-1.11 for MIROC. At present, the effect of climate change on hurricane size has not been investigated; therefore, it is unclear whether the surge will greatly increase due to the simultaneous increase in storm intensity and size or only moderately change when one factor increases while the other decreases. Further investigation of the storm size distribution under different climates is needed to answer this question.

Discussion

As the climate warms, the global mean sea level is projected to rise, due to thermal expansion and melting of land ice. Superimposed on the global SLR, regional sea levels may change due to local land subsidence and ocean circulation changes, both of which are expected to significantly increase sea level in the NYC area[45, 46]. The total SLR for NYC is projected to be in the range of 0.5-1.5 m by the end of the century[21, 40, 47]. The effect of SLR, rather than changes in storm characteristics, has been the focus of most studies on the impact of climate change on coastal flooding risk (e.g., refs. 45 and 48); some studies also account for the change of hurricane intensity due to the change of the sea surface temperature (e.g., refs. 49 and 50). To our knowledge, this paper is the first to explicitly simulate large numbers of hurricane surge events

under projected climates to assess surge probability distributions. Our study shows that some climate models predict the increase of the surge flooding level due to the change of storm climatology to be comparable to the projected SLR for NYC. For example, the CNRM and GFDL models predict that, by the end of the century, the 100-year and 500-year storm tide levels will increase by about 0.7-1.0 m (Figs. 3a and 3c). More consequential, the combined effect of storm climatology change and SLR will greatly shorten the surge flooding return periods. As shown by the estimated flood return level in Fig. 4, if we assume the SLR in the NYC area to be 1 m, by the end of the century, the current NYC 100-year surge flooding may occur every 20 years or less (with CNRM, GFDL, ECHAM, and MIROC yielding predictions of 4/4, 3/3, 21/20, and 14/13 years, respectively, for observed/increased storm sizes), the current 500-year surge flooding may occur every 240 years or less (with CNRM, GFDL, ECHAM, and MIROC yielding predictions of 62/29, 28/24, 188/140, and 241/173 years, respectively). These findings are dependent on the climate models used to generate the environmental conditions for the storm simulations, so other climate models may produce different results. Nevertheless, all four climate models used in this study predict significant increases in the surge flood level due to climate change, providing an additional rationale for a comprehensive approach to managing the risk of climate change, including long-term adaptation planning and greenhouse-gas emissions mitigation.

Methods

High-resolution surge simulations are computationally intensive; therefore, to make it possible to simulate surges with reasonable accuracy for our large synthetic storm sets, we apply the two

hydrodynamic models with numerical grids of various resolutions in such a way that the main computational effort is concentrated on the storms that determine the risk of concern. First, the SLOSH simulation, using a polar grid with resolution of about 1 km around NYC, is applied as a filter to select the storms that have return periods, in terms of the surge height at the Battery, greater than 10 years, the typical range of hurricane surge periodicity relevant to design and policy-making. Second, the ADCIRC simulation, using an unstructured grid with resolution of ~100 m around NYC (and up to 100 km over the deep ocean), is applied to each of the selected storms (see Supplementary Fig. S1, for a comparison between SLOSH and ADCIRC simulations). To determine whether the resolution of the ADCIRC simulation is sufficient, another ADCIRC mesh[30] with resolution as high as ~10 m around NYC is used to simulate over 200 most extreme events under the observed climate condition. The differences between the results from the two grids are very small, with our ~100-m mesh overestimating the surge at the Battery by about 2.5% (Fig. S2). Thus, the ~100-m ADCIRC simulations are used, with a 2.5% reduction, to estimate the surge levels at the Battery for return periods of 10 years and longer. (ADCIRC model control parameters follow refs. 29 and 30, whose results have been validated against observations.)

To quantify tide-surge nonlinearity, we generate a database of the storm surge and storm tide for over 200 most extreme events arriving every 3 hours during a tidal cycle. We model the nonlinearity (denoted by L: the difference between simulated storm tide, surge, and astronomical tide) as a function of the tidal phase (φ) when the (peak) surge arrives, the surge height (H), tidal range (t_r), and mean tidal level (t_m). We define a non-dimensional factor γ for the nonlinearity as

$$\gamma = \frac{L+t_m}{H+t_r} \ , \qquad (1)$$

294 so that, for a given value of γ, the higher the storm surge or the astronomical tide, the larger the
295 nonlinearity relative to the negative mean tidal level ($-t_m$; considering that the nonlinearity and
296 the tide are out of phase, Fig. S4). We use the generated storm surge and storm tide database to
297 estimate γ by kernel regression as a function of the tidal phase (Fig. S5). Then, the nonlinearity
298 L, for a given tide and a surge H corresponding to tidal phase φ, is estimated as

299 $$L(\varphi) = \gamma(\varphi)(H + t_r) - t_m. \quad (2)$$

300

301 We assume the annual number of NY-region storms to be Poisson-distributed, with mean λ.
302 The probability distribution of surge height H, $P\{H<h\}$, is estimated from the generated surges
303 for each storm set. The surge PDF is applied to estimate the PDF of the storm tide (H^t),

304 $$P\{H^t < h\} = P\{H + t(\Phi) + L(\Phi) < h\} \quad (3)$$

305 where t is the height of the astronomical tide and Φ is the (random) phase when the storm surge
306 arrives. Making use of the estimated γ function, equation (3) becomes

307 $$P\{H^t < h\} = \int_0^{2\pi} P\{H < \frac{h - t(\varphi) - \gamma(\varphi)t_r + t_m}{1+\gamma(\varphi)}\} P\{\Phi = d\varphi\}, \quad (4)$$

308 It is reasonable to assume that the surge can happen at any time during a tidal cycle with
309 equal likelihood, and equation (4) becomes

310 $$P\{H^t < h\} = \int_0^{2\pi} P\{H < \frac{h - t(\varphi) - \gamma(\varphi)t_r + t_m}{1+\gamma(\varphi)}\} \frac{1}{2\pi} d\varphi . \quad (5)$$

311 (Note that equation (5) can be extended to include the effects of different tides during the
312 hurricane season by taking a weighted average of $P\{H^t<h\}$ for all types of tides considered,
313 with weights equal to the fractions of time during the season when different types of tide
314 occur.) Then, by definition, storm tide return period T^t is

315 $$T^t = \frac{1}{1 - e^{-\lambda(1 - P\{H^t < h\})}} . \quad (6)$$

No analytical expression for the return level (h) is available in this case; the storm tide return levels in Figs. 2 and 3 are calculated by solving equations (5) and (6) numerically. We used the astronomical tide cycle observed at the site during the period of Sep. 18-19, 1995 (NOAA tides and currents), assuming the tidal variation at NYC during the hurricane season is relatively small.

The surge PDF is also applied to estimate the PDF of the flood height (H^f),

$$P\{H^f < h\} = P\{H + t(\Phi) + L(\Phi) + S < h\}\,, \tag{7}$$

where S is the SLR, and the nonlinear effect of SLR on the surge is neglected. Then, based on equation (5),

$$P\{H^f < h\} = \int_0^{s_m} \int_0^{2\pi} P\{H < \frac{h - t(\varphi) - \gamma(\varphi) t_r + t_m - s}{1+\gamma(\varphi)}\} P\{S = ds\} \frac{1}{2\pi} d\varphi\,, \tag{8}$$

where it is assumed that the range of possible SLR is [0, s_m]. The probability distribution of SLR may be estimated from GCM simulations and/or other methods[21, 47]. It is also useful to estimate the flood return level for a certain SLR. For a given SLR (s), equation (8) reduces to

$$P\{H^f < h\} = \int_0^{2\pi} P\{H < \frac{h - t(\varphi) - \gamma(\varphi) t_r + t_m - s}{1+\gamma(\varphi)}\} \frac{1}{2\pi} d\varphi\ . \tag{9}$$

The flood return period T^f is

$$T^f = \frac{1}{1 - e^{-\lambda(1 - P\{H^f < h\})}}\ . \tag{10}$$

The flood return levels in Fig. 4 are calculated by solving equations (9)-(10) numerically, assuming a SLR of 1 m (s=1) for the future climate (and s= 0 for the current climate) and using the astronomical tide cycle observed during Sep. 18-19, 1995. The statistical confidence interval of the estimated storm tide and surge flood return levels remains the same as the confidence interval of the estimated surge return level, as no new distribution parameters are introduced. The

uncertainty in the estimation of the future return levels may be considered as the combination of the statistical confidence interval and the variation of predictions from different climate models.

Please contact Ning Lin (ninglin@mit.edu) for correspondence and requests for materials.

Acknowledgments N.L. was supported by the NOAA Climate and Global Change Postdoctoral Fellowship Program, administered by the University Corporation for Atmospheric Research, and the Princeton Environmental Institute and the Woodrow Wilson School of Public and International Affairs for the Science, Technology and Environmental Policy (STEP) fellowship. We thank Professor Joannes Westerink and Dr. Seizo Tanaka of the University of Notre Dame for their great support on the ADCIRC implementation. We also thank Professor Brian Colle of Stony Brook University for providing us with the high-resolution ADCIRC mesh.

Author contributions All authors contributed extensively to the work presented in this paper, and all contributed to the writing, with N.L. being the lead author.

Additional information The authors declare no competing financial interests. Supplementary information accompanies this paper on www.nature.com/nclimate. Correspondence and requests for materials should be addressed to N.L. (ninglin@mit.edu).

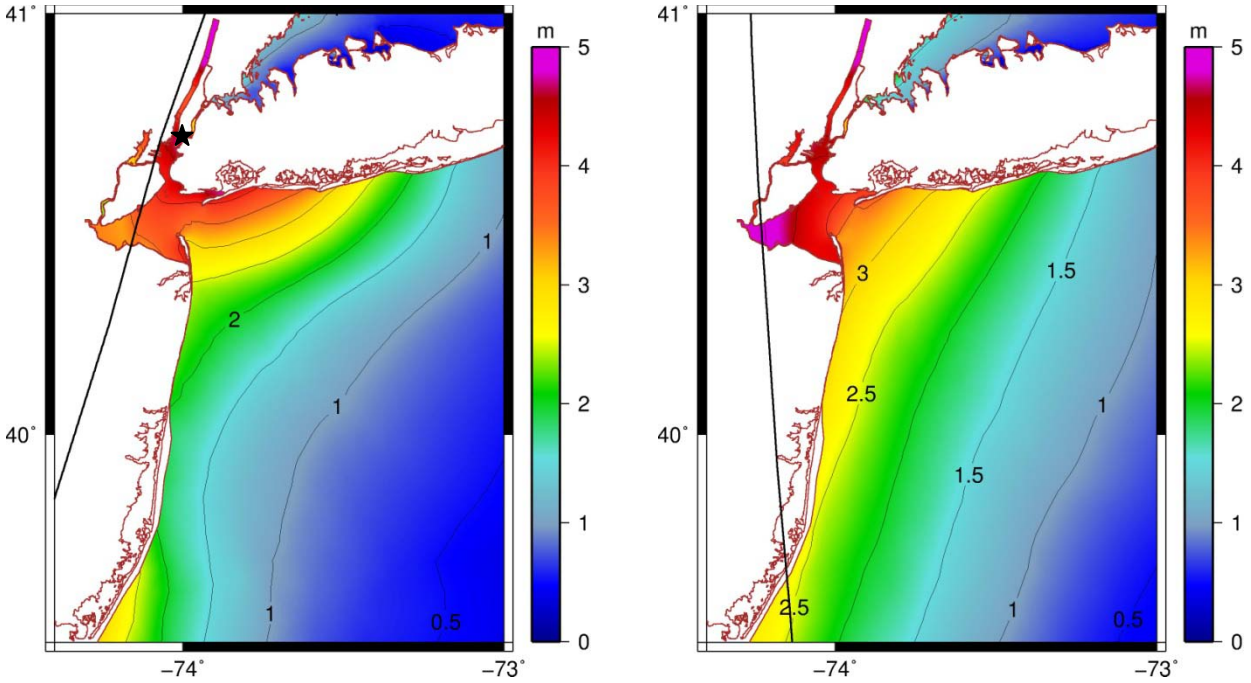

Figure 1. Two worst-case surge events for the Battery (generated by the ADCIRC simulations with resolution of ~100 m around NYC), under the NCAR/NCEP current climate. The contours and colors show the maximum surge height (m) during the passage of the storm. The black curve shows the storm track. The black star shows the location of the Battery. The storm parameters when the storm is closest to the Battery site are: (a). storm symmetrical maximum wind speed V_m = 56.6 m/s, minimum sea-level pressure P_c = 960.1 mb, radius of maximum wind R_m = 39.4 km, translation speed U_t = 15.3 m/s, and distance to the site ds = 3.9 km; (b). V_m = 52.1 m/s, P_c = 969.2 mb, R_m = 58.9 km, U_t = 9.7 m/s, and ds = 21.1 km.

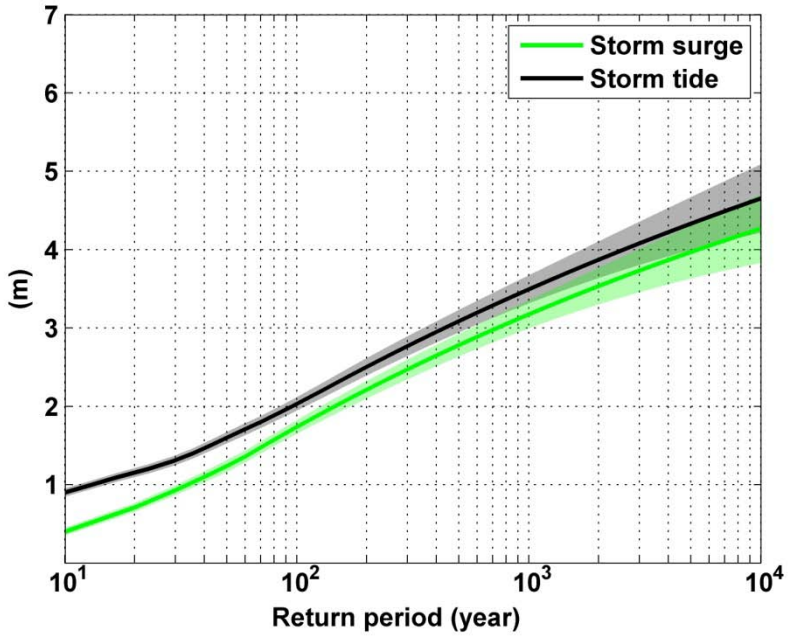

Figure 2. Estimated return levels for the Battery of the storm surge (m; green) and storm tide (m; black) for the NCAR/NCEP current climate. The shade shows the 90% confidence interval.

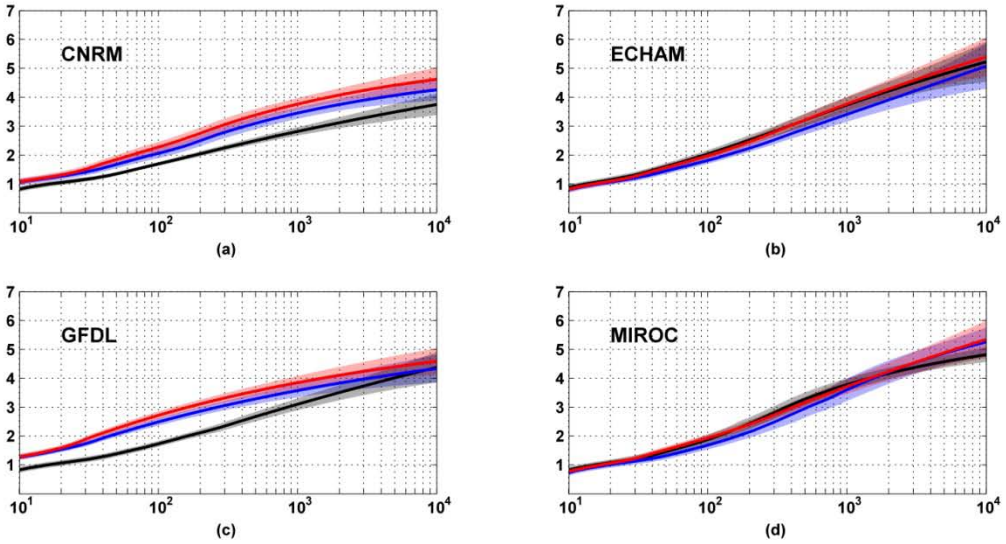

377

378

379 Figure 3. Estimated storm tide return levels for the current climate (black), the IPCC A1B
380 climate (blue), and the IPCC A1B climate with R_o increased by 10% and R_m by 21% (red),
381 predicted by each of the four climate models. The x axis is the return period (year) and the y axis
382 is the storm tide (m) at the Battery. The shade shows the 90% confidence interval.

383

384

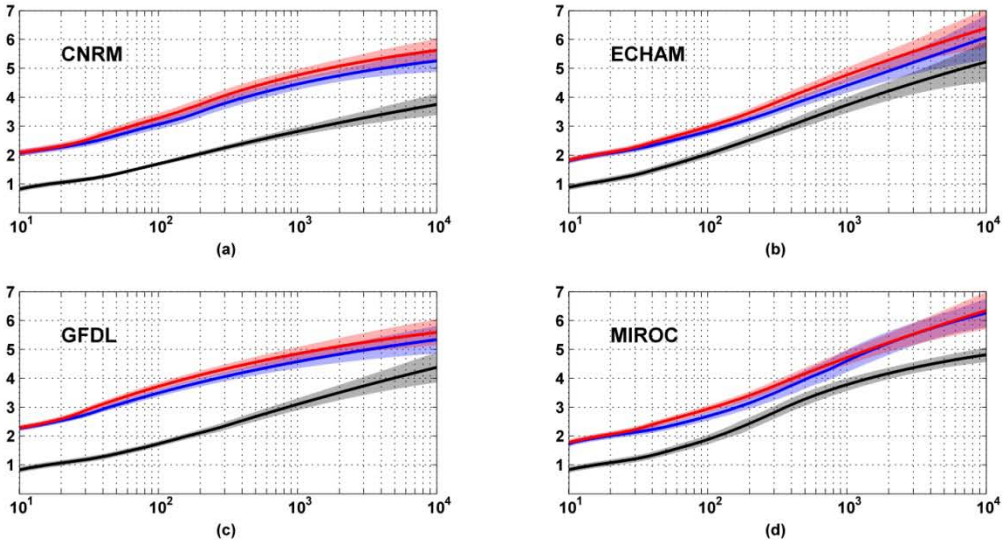

Figure 4. Estimated flood return levels for the current climate (black), the IPCC A1B climate (blue), and the IPCC A1B climate with R_o increased by 10% and R_m by 21% (red), predicted by each of the four climate model. The SLR for the A1B climate is assumed to be 1 m. The x axis is the return period (year) and the y axis is the flood height (m) at the Battery. The shade shows the 90% confidence interval.

398 References

[1] Emanuel, K. The dependence of hurricane intensity on climate. *Nature*, **326**, 2, 483-485 (1987).

[2] Emanuel, K. The hurricane–climate connection. *Bull. Am. Meteorol. Soc.* **5**, ES10–ES20 (2008).

[3] Bender, M. A. et al. Model impact of anthropogenic warming on the frequency of intense Atlantic hurricanes. *Science*, **327**, 454–458 (2010).

[4] Knutson, T. R. et al. Tropical cyclones and climate change. *Nature Geosci.,* **3.3**, 157-163 (2010).

[5] Powell, M. D. & Reinhold, T. A. Tropical cyclone destructive potential by integrated kinetic energy. *Bull. Amer. Meteor. Soc.,* **88,** 513–526 (2007).

[6] Resio, D.T. & Westerink, J. J. Hurricanes and the physics of surges. *Physics Today,* **61**, 9, 33-38 (2008).

[7] Rego, J. L. & Li, C. On the importance of the forward speed of hurricanes in storm surge forecasting: A numerical study. *Geophys. Res. Lett.,* **36,** L07609 (2009). doi:10.1029/2008GL036953

[8] Irish, J. L. & Resio, D. T. A hydrodynamics-based surge scale for hurricanes. *Ocean Eng.*, **37**, 1, 69-81 (2010).

[9] Irish, J. L., Resio, D.T. & Ratcliff, J.J. The Influence of storm size on hurricane surge. *J. Phys. Oceanogr.,* **38**, 2003–2013 (2008). doi: 10.1175/2008JPO3727.1

[10] Resio, D.T., Irish, J.L. & Cialone, M.A. A surge response function approach to coastal hazard assessment – part 1: basic concepts. *Natural Hazards,* **51**, 1, 163-182 (2009). doi: 10.1007/s11069-009-9379-y

[11] Irish, J. L., Resio, D.T. & Ratcliff, J.J. The Influence of Storm Size on Hurricane Surge. *J. Phys. Oceanogr.,* **38**, 2003–2013 (2008), doi: 10.1175/2008JPO3727.1.

[12] Knutson, T.R, Sirutis, J.J., Garner, S.T., Held, I.M. & Tuleya, R.E. Simulation of the recent multidecadal increase of atlantic hurricane activity using an 18-km-grid regional model. *Bull. Am. Meteorol. Soc.,* **88**, 1549–1565 (2007). doi:10.1175/BAMS-88-10-1549

[13] Knutson, T.R, Sirutis, J.J., Garner, S.T., Vecchi, G.A. & Held, I.M. Simulated reduction in Atlantic hurricane frequency under twenty-first-century warming conditions. *Nat. Geosci.,* **1**, 359–364 (2008). doi:10.1038/ngeo202

[14] Nicholls, R.J. Coastal megacities and climate change. *GeoJournal,* **37**, 3, 369-379 (1995). doi: 10.1007/BF00814018

[15] Rosenzweig, C. & Solecki, W. Chapter 1: New York City adaptation in context. *Ann. N.Y. Acad. Sci.,* ***1196***, 19-28 (2010). doi: 10.1111/j.1749-6632.2009.05308.x

[16] Rosenzweig, C., Solecki, W., Hammer, S.A. & Mehrotra, S. Cities lead the way in climate–change action. *Nature,* **467**, 909–911 (2010). doi:10.1038/467909a

[17] Emanuel, K., Ravela, S., Vivant, E. & Risi, C. A Statistical deterministic approach to hurricane risk assessment. *Bull. Amer. Meteor. Soc.*, **87**, 299-314 (2006).

[18] Emanuel, K., Sundararajan, R. & Williams, J. Hurricanes and global warming: results from downscaling IPCC AR4 simulations. *Bull. Am. Meteor. Soc.,* **89**, 347–367 (2008).

[19] Emanuel, K., Oouchi, K., Satoh, M., Hirofumi, T. & Yamada, Y. Comparison of explicitly simulated and downscaled tropical cyclone activity in a high-resolution global climate model. *J. Adv. Model. Earth Sys.,* **2**, 9 (2010). doi:10.3894/JAMES.2010.2.9

[20] Kalnay, E. et al. The NCEP/NCAR 40-year reanalysis project. *Bull. Amer. Meteor. Soc.*, **77**, 437-471 (1996).

[21] Solomon, S. et al., Eds. *Climate Change 2007: The Physical Science Basis.* (Cambridge University Press, 2007).

[22] Jarvinen, B. R., Neumann, C. J. & Davis, M. A. S. A Tropical Cyclone Data Tape for the North Atlantic Basin, 1886–1983: Contents, Limitations, and Uses. NOAA Tech. Memo NWS NHC 22 (NOAA/Tropical Prediction Center, Miami, Fla. 1984).

[23] Villarini, G., Vecchi, G.A., Knutson, T. R., Zhao, M., Smith, J. A. North Atlantic Tropical Storm Frequency Response to Anthropogenic Forcing: Projections and Sources of Uncertainty. *J. Climate*, **24**, 3224–3238 (2011). doi: 10.1175/2011JCLI3853.1

[24] Luettich R.A., Westerink, J.J. & Scheffner, N.W. *ADCIRC: An Advanced Three-dimensional Circulation Model for Shelves, Coasts and Estuaries, Report 1: Theory and Methodology of ADCIRC-2DDI and ADCIRC-3DL*. DRP Technical Report DRP-92-6. (Department of the Army, US Army Corps of Engineers, Waterways Experiment Station, Vicksburg, MS, 1992).

[25] Westerink, J.J., Luettich, R.A., Blain, C.A. & Scheffner, N.W. *ADCIRC: An Advanced Three-Dimensional Circulation Model for Shelves, Coasts and Estuaries; Report 2: Users Manual for ADCIRC-2DDI*. (Department of the Army, US Army Corps of Engineers, Washington D.C., 1994).

[26] Jelesnianski, C. P., Chen, J. & Shaffer, W. A. *SLOSH: Sea, lake, and Overland Surges from Hurricanes*. (NOAA Tech. Report NWS 48, 1992).

[27] Jarvinen, B. R. and Lawrence, M. B. Evaluation of the SLOSH storm-surge model. *Bull. Am. Meteor. Soc.,* **66**, 11, 1408-1411 (1985).

[28] Jarvinen, B. & Gebert, J. *Comparison of Observed versus SLOSH Model Computed Storm Surge Hydrographs along the Delaware and New Jersey Shorelines for Hurricane Gloria, September 1985*. (U.S. Department of Commerce, National Hurricane Center, Coral Gables, FL. 1986).

[29] Westerink, J. J., et al. A basin- to channel-scale unstructured grid hurricane storm surge model applied to southern Louisiana. *Mon. Weather Rev.,* **136**, 833-864 (2008). doi:10.1175/2007MWR1946.1

[30] Colle, B. A. et al. New York City's vulnerability to coastal flooding. *Bull. Am. Meteorol. Soc.,* **89**, 829-841 (2008). doi:10.1175/2007BAMS2401.1

[31] Lin, N., Smith, J. A., Villarini, G., Marchok, T. P. & Baeck, M. L. Modeling extreme rainfall, winds, and surge from Hurricane Isabel (2003). *Wea. Forecasting*, **25**, 1342–1361 (2010). doi: 10.1175/2010WAF2222349.1

[32] Dietrich J.C. et al. Modeling hurricane waves and storm surge using integrally-coupled, scalable computations. *Coast. Eng.,* **58**, 1, 45-65 (2011).

[33] Emanuel, K. & Rotunno, R. Self-Stratification of tropical cyclone outflow. Part I: Implications for storm structure. *J. Atmos. Sci.,* in press (2011).

[34] Georgiou, P.N., Davenport, A.G. & Vickery, B.J. Design windspeeds in regions dominated by tropical cyclones. *J. Wind Eng. Ind. Aerodyn.*, **13,** 139–159 (1983).

[35] Bretschneider, C.L. A non-dimensional stationary hurricane wave model. *Proceedings of the Offshore Technology Conference, Houston, Texas*, **I**, 51–68 (1972).

[36] Holland, G.J. An analytic model of the wind and pressure profiles in hurricanes. *Mon. Weather Rev.*, **108**, 1212-1218 (1980).

[37] Scileppi, E. & Donnelly, J. P. Sedimentary evidence of hurricane strikes in western Long Island, New York. *Geochem. Geophys. Geosyst.* **8**, 1–25 (2007)

[38] Coles, S. *An Introduction to Statistical Modeling of Extreme Values*. (Springer, London, 2001).

[39] Lin, N., Emanuel, K. A., Smith, J. A. & Vanmarcke, E. Risk assessment of hurricane storm surge for New York City. *J. Geophys. Res.*, **115,** D18121 (2011). doi:10.1029/2009JD013630

[40] Rosenzweig, C., & Solecki W. (Eds.) *Climate Risk Information, Report for the New York City Panel on Climate Change*. (Columbia Earth Inst, New York, 2009).

[41] Colle, B. A., Rojowsky, K. and Buonaiuto, F. New York City storm surges: Climatology and analysis of the wind and cyclone evolution. *J. Appl. Meteor. and Climatology*, **49**, 85-100 (2010).

[42] Chavas, D. R. & Emanuel, K. A. A QuikSCAT climatology of tropical cyclone size. *Geophys. Res. Lett.,* **37**, L18816 (2010). doi:10.1029/2010GL044558

[43] Emanuel, K. A. An air-sea interaction theory for tropical cyclones. Part I: Stady-state maintenance. *J. Atmos. Sci.*, **43**, 585-605 (1986).

[44] Emanuel, K. Environmental Factors Affecting Tropical Cyclone Power Dissipation. *J. Climate*, **20**, 5497–5509 (2007). doi: 10.1175/2007JCLI1571.1

[45] Gornitz, V., Couch, S. & Hartig, E. K. Impacts of sea level rise in the New York City metropolitan area. *Global and Planet. Change* **32**, 1, 61-88 (2001).

[46] Yin, J., Schlesinger, M.E. & Stouffer, R.J. Model projections of rapid sea-level rise on the northeast coast of the United States. *Nature Geosci.,* **2**, 262-266 (2009).

[47] Horton, R., Gornitz, V., and Bowman M. Chapter 3: Climate observations and projections. *Ann. N.Y. Acad. Sci.*, **1196,** 41-62 (2010).

[48] Hunter, J. Estimating sea-level extremes under conditions of uncertain sea-level rise. *Climatic Change*, **99**, 331-350 (2010).

[49] Mousavi, M. E., Irish, J. L., Frey, A.E., Olivera, F. & Edge, B. L. Global warming and hurricanes: the potential impact of hurricane intensification and sea level rise on coastal flooding. *Climatic Change,* **104**, 3-4, 575-597 (2010). doi: 10.1007/s10584-009-9790-0

[50] Hoffman, R. N. et al. An estimate of increases in storm surge risk to property from sea level rise in the first half of the twenty-first century. *Wea. Climate Soc.*, **2**, 271–293 (2010). doi: 10.1175/2010WCAS1050.1